CHEMISTRY OF MATERIALS

pubs.acs.org/cm

Article

Size-Dependent PbS Quantum Dot Surface Chemistry Investigated via Gel Permeation Chromatography

Adam Roberge, John H. Dunlap, Fiaz Ahmed, and Andrew B. Greytak*

Cite This: *Chem. Mater.* 2020, 32, 6588–6594

Read Online

ACCESS | Metrics & More | Article Recommendations | Supporting Information

ABSTRACT: We report the first comprehensive study on the purification of PbS quantum dots (QDs) using gel permeation chromatography (GPC). GPC enables the efficient and repeatable separation of unbound small molecules from QDs in a homogeneous solvent environment. This separation allows us to gain further insight into the surface capping layer of PbS QDs and measure the ligand density on QDs of different sizes. We find that small oleate-capped PbS QDs are stable in solution in toluene after purification by GPC with negligible free ligand concentrations. However, purification of larger-diameter QDs reveals two oleate populations that persist after multiple GPC purifications: one with a broad olefin resonance characteristic of strongly bound ligands in smaller QDs, and the other with a narrower peak suggesting dynamic exchange with freely diffusing species. Variable-temperature NMR indicates a reversible equilibrium between the two populations, which is also observed in samples purified through precipitation with a polar solvent. The observation of two oleate populations following GPC purification is maintained even when the large-diameter QDs are formed using a strictly anhydrous procedure that should eliminate the presence of water, hydroxide, or oleic acid in as-synthesized samples. In conducting this strictly anhydrous synthesis, we incidentally observe that water plays a role in determining the resultant size of PbS QDs prepared by traditional methods compared to their anhydrous analogues. Understanding how the surfaces of PbS QDs are terminated should aid in interpreting their behavior in subsequent ligand exchange steps as necessary for diverse applications.

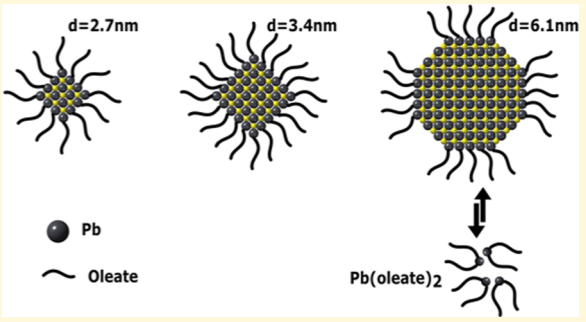

INTRODUCTION

Semiconductor nanocrystal quantum dots (QDs) have commanded considerable interest due to their unique size-tunable optical properties and solution processability. However, because of their size, QDs inherently possess large surface-to-volume ratios, and it has been shown that many, if not all, of the desirable properties can be altered by surface modification. Therefore, it is paramount to understand and care for the surfaces of these particles to achieve the desired optoelectronic properties. Lead sulfide (PbS) QDs have undergone extensive research as their band gap energy and large Bohr radius have made them favorable targets for a variety of optoelectronic applications. These include photovoltaics, for which the effective band gap can be tuned for single-junction devices or made to match up with silicon in tandem cell designs and IR sensors.[1−3] Additionally, synthetic methods have been discovered to form PbS QDs with low dispersities in radius over wide a range of sizes.[4−7] Typically, to achieve size control, good size distribution, and colloidal stability, long-chain, primarily aliphatic ligands are used during the synthesis. These ligands, while necessary for synthesis, are often exchanged with short-chain molecules that increase charge transport in films. To optimize such ligand exchange reactions, for example, to reduce an excess of unused new ligand, knowledge of what the as-synthesized ligand layer is, as well as the quantity of ligands present after synthesis, is beneficial.

Several reports have described the ligand density on PbS quantum dots; in these studies, the main purification method employed has been precipitation with a polar solvent followed by redissolution (PR).[8−11] For example, Grisorio et al. examined ligand populations on a size series of oleate-capped PbS QDs isolated by PR via NMR.[8] Beygi et al. compared the ligand weight percentage determined by elemental analysis to predictions based on octahedral and cuboctahedral atomistic models in which Pb-saturated (111) facets were coordinated by oleate.[9] Kessler and Dempsey examined displacement of lead oleate ($Pb(OA)_2$) ligands from PbS QDs on exposure to a chelating nucleophile.[11] Although PR is the most common purification method for semiconductor nanocrystals, it has been demonstrated previously that it can be detrimental to the particles due to changes in the solvent environment.[12] As a

Received: May 13, 2020
Revised: July 16, 2020
Published: July 16, 2020

https://dx.doi.org/10.1021/acs.chemmater.0c02024
Chem. Mater. 2020, 32, 6588–6594

size-based separation process, gel permeation chromatography (GPC) is an alternative approach to isolating QDs while maintaining the solvent environment.[13,14] GPC purification of PbS QDs before and after ligand exchange has been reported recently by our group and others,[15,16] but the quantification of the ligand layer was not investigated.[15]

Herein, we describe the use of GPC to purify oleate-capped PbS QDs, synthesized by the Hines method,[4,5] of a range of sizes, and determine the ligand density. We find that GPC purification of PbS QDs leads to repeatable ligand layers and stable QD solutions. Though the number of ligands per QD increases with increasing size, the density per unit surface area decreases at larger sizes. While investigating the possible role of adventitious water in determining surface termination in oleate-capped QDs, we observed a significant difference in the ultimate size when anhydrous lead oleate was used as the precursor in place of that prepared directly from hydrolysis of PbO with oleic acid. We note that while Hendricks et al. implemented dry $Pb(OA)_2$ as a precursor for PbS QDs in combination with substituted thiourea sulfur sources,[17] the influence of adventitious water on size in the Hines synthesis, where bistrimethylsilylsulfide ($(TMS)_2S$) is the sulfur source, has not been described previously.

EXPERIMENTAL SECTION

Materials. All materials were used as received without further purification. Lead(II) oxide (PbO, 99.9%), oleic acid (OAH, 90%), acetonitrile (anhydrous, 99.8%), trifluoroacetic acid (99%), trifluoroacetic anhydride (>99%), and triethylamine (99%) were purchased from Alfa Aesar. 1-Octadecene (ODE, 90%), bistrimethylsilylsulfide ($(TMS)_2S$, 95%), and ferrocene (98%) were purchased from Acros Organics. Toluene and isopropanol (certified ACS) were purchased from Fisher Chemical. Toluene-d_8 was purchased from Cambridge Isotope Laboratories. *n*-Octane was purchased from EMD Millipore. Biobeads S-X1 medium (column stationary phase, 14 000 MWCO) was purchased from Bio-Rad. Methyl acetate was purchased from VWR and dried over 4A molecular seives.

PbS QD Synthesis. Quantum dots were synthesized using the method described by Zhang et al.[5] In brief, PbO, OAH, and ODE were combined in a 50 mL three-neck round-bottom flask and heated in vacuo to 100 °C. After switching to N_2 atmosphere, a solution of $(TMS)_2S$ in ODE was injected at 95 °C and allowed to cool to room temperature. The crude synthesis solution was then collected, and acetone (or dried methyl acetate for anhydrous samples) was used to precipitate the QDs. After centrifugation at 5000 rpm for 5 min, the supernatant was discarded, and the precipitate dissolved in neat toluene. The solutions were stored in toluene until further analysis. Anhydrous lead oleate ($Pb(OA)_2$) was synthesized using a modified procedure from Hendricks et al.[17] In brief, lead trifluoroacetate was synthesized using lead(II) oxide, trifluoroacetic acid, and trifluoroacetic anhydride in acetonitrile solvent. Separately, oleic acid and triethylamine were combined in isopropanol solvent. The addition of lead trifluoroacetate to the oleic acid solution formed a white precipitate. The precipitate was isolated using vacuum filtration, washed with methanol, dried using a Schlenk line, and transferred into a nitrogen glovebox.

Gel Permeation Chromatography. GPC purification of QDs was conducted as described previously, using a bed height of approximately 140 mm.[13] Using a toluene mobile phase, the elution time for the QDs was 10 ± 1 min.

Characterization. Absorbance measurements were recorded using a Cary 5000 ultraviolet−visible−near-infrared (UV−vis−NIR) spectrometer. For these measurements, aliquots of PbS QDs were diluted into *n*-octane. GPC purification was performed on ∼100 nmol quantities of QDs. The collected eluent was then pumped dry on a Schlenk line and dissolved to ca. 100 μM in toluene-d_8 with ferrocene as an internal standard. ^{1}H NMR was performed on a Bruker Avance III 400 MHz using 32 scans with a 30 s T_1 delay, except for variable-temperature (VT) NMR recorded using a Bruker Avance III 500 MHz spectrometer. Ligand populations in VT-NMR samples were analyzed using Mestre Nova 14.11 software by fitting the oleate olefin resonance with as a sum of two peaks with variable Gaussian and Lorentzian contributions.

RESULTS AND DISCUSSION

PbS QD Ligand Density as Function of Size. We synthesized PbS QDs using methods initially described by Hines et al., and more recently detailed by Zhang et al. for accessing a range of QD sizes.[4,5] The measured absorbance spectra (Figure 1), in combination with sizing curves published

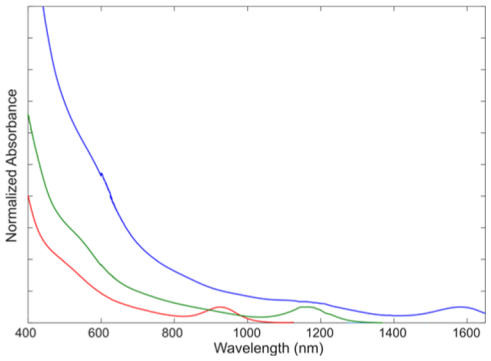

Figure 1. Normalized absorbance spectra of PbS QDs normalized to 1s peak intensity.

by Moreels et al., were used to calculate the size and concentration of the PbS QDs.[18] The QD sizes used in this study ranged from 2.7 to 6.1 nm in diameter. After synthesis, an initial solvent change from 1-octadecene (ODE) to toluene was effected by one cycle of precipitation and redissolution. The QDs were then purified using GPC in the toluene mobile phase with a polystyrene gel as the stationary phase. As shown in Figure 2, removal of residual ODE and unbound oleate ligands can be observed clearly in ^{1}H NMR spectra of samples before and after the GPC purification step (Figure 2). This result, which is achieved with no apparent changes in the electronic absorbance spectra (Figure S1), confirms the validity of GPC purification as a method to purify PbS QDs. We note that loading PbS QDs onto the column in a pure ODE solvent is unsatisfactory due to its high viscosity and because it is not as good a solvent for the polystyrene gel. Purification of PbS QDs without any precipitation and redissolution step can be achieved by dilution of the as-synthesized stock solution in toluene prior to loading, or by removing a majority of the ODE under high vacuum. Here, we used one cycle of PR to bring the QDs into toluene prior to GPC to increase the amount of QDs that could be purified in a single run of the column. As can be seen in Figure 2A, ODE and excess oleate species remain present after the initial PR, and indeed multiple PR cycles are typically required to prepare PbS QDs for optoelectronic applications.[10,19] These additional cycles can be eliminated through the use of GPC.

To determine ligand populations in PbS QD samples, ferrocene (Fc) was employed as an internal standard in ^{1}H NMR. The total concentration of oleate species [OA] was calculated from the relative strength of the olefin proton resonance

https://dx.doi.org/10.1021/acs.chemmater.0c02024
Chem. Mater. 2020, 32, 6588−6594

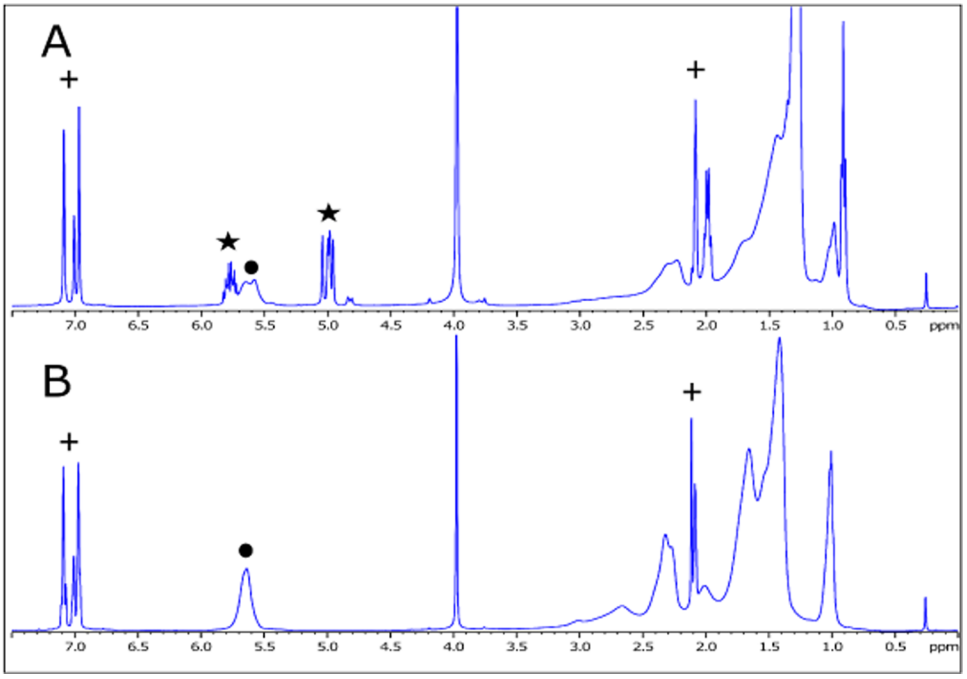

Figure 2. ^{1}H NMR of PbS QDs before (A) and after (B) GPC purification. Peaks from growth solvent (★) are removed after purification leaving bound oleate ligands (●). Toluene peaks are indicated by (+); peak at $\delta \approx 4$ ppm is Fc internal standard.

$$[\mathrm{OA}] = [\mathrm{Fc}] \times \frac{10}{\int \mathrm{Fc}} \times \frac{\int \mathrm{Olefin}}{2}$$

By dividing [OA] by the concentration of QDs as determined from the absorbance, a ratio of oleate/QD could be obtained. For comparison among QD samples of varying radius, the oleate ligand population can be expressed as a density per unit area using an assumption of pseudospherical particles. Our results, compiled from three independent GPC purification runs in each case, are listed in Table 1 for the size range tested.

Table 1. Ligand Population and Density for PbS QDs of Varying Sizes

1s peak (nm)	diameter (nm)	OA/QD	OA (nm^{-2})	ligand (wt %)
925	2.77	111 ± 1	4.63 ± 0.06	38.0
1142	3.38	153 ± 1	4.23 ± 0.08	31.8
1584	6.12	494 ± 48	4.20 ± 0.41	20.2

The ligand density decreases with increasing QD size over the size ranges tested. This can be understood partly as a relaxed steric constraint in small particles due to the greater volume available per ligand on surfaces of high convex curvature. However, charge balance must also be considered as oleate ligands on PbS QDs are generally compensated by excess Pb^{2+} ions on the surface (compared to the bulk PbS stoichiometry). Choi et al. showed that oleate-capped PbS QDs undergo a sterically driven shape transition that changes the shape of the particle from octahedral to truncated octahedral as the diameter increases.[20] Though ligand populations were not directly measured, based on Pb/S elemental ratios, they found that at sizes less than 4 nm in diameter, the QD is primarily terminated by Pb rich (111) facets, but as the size increases neutral (100) facets begin to appear. On a Pb-saturated (111) facet, half of the Pb atoms exist in excess of the 1:1 stoichiometry of bulk PbS. Charge balance can be satisfied by placing one anionic ligand per Pb atom, such that the ligands represent formula equivalents of $Pb(oleate)_2$; however, the atom density of 6.55 nm^{-2} on the (111) facet appears to exceed the density at which oleate ligands can pack on a bulk planar surface as noted by Choi and others.[20,21]

For comparison to previous studies of ligand populations such as Beygi et al.,[9] we can estimate the ligand weight percentage in our samples, considering the mass of a PbS sphere of the size noted and the ligand equivalency per QD from NMR. In a representative sample, the ligand weight percentage obtained this way closely matched the mass loss on heating in thermogravimetric analysis (Figure S2). The NMR-derived weight percentages for our size series of GPC-purified QDs are listed in Table 1, and they agree quite well with Beygi et al.'s results for the two smaller sizes. The NMR ligand ratios for the two smaller sizes in Table 1 are also in close agreement with NMR-derived oleate ratios reported by Kessler and Dempsey in a recent report on ligand displacement in PbS QDs.[11] Our largest size of 6 nm was not explored experimentally by Beygi or Kessler. Beygi et al. considered that neutral oleic acid could coordinate 100 facets on truncated octahedral QDs, leading to a total ligand density ~6 nm^{-2}. However, we do not observe an OH stretch in the Fourier transform infrared (FTIR) spectra of GPC-purified samples as might be expected for oleic acid (Figure S3), and the total density of strongly bound OA associated with the broadened olefin NMR peak is significantly smaller at 4.20 ± 0.41 nm^{-2}. For a regular truncated octahedron, (111) facets account for about 77% of the total surface area. Our results suggest either diminished (111) facet coverage or incompletely Pb-polar (111) facets, at the 6 nm size.

Size-Dependent Dynamic Ligand Population. While the NMR result in Figure 2 is typical for smaller PbS QDs, GPC purification of the largest-size QDs (6.12 nm) revealed interesting ligand behavior observable in ^{1}H NMR (Figure S4).

https://dx.doi.org/10.1021/acs.chemmater.0c02024
Chem. Mater. 2020, 32, 6588−6594

After GPC purification, two olefin populations are observed by ^{1}H NMR. Frequently, ligand binding to a nanocrystal is associated with the broadening of NMR peaks, primarily due to slower rotational diffusion of the bound ligand compared to the free ligand. Therefore, it is possible to differentiate bound ligand from free ligand in the NMR. Previously, our group has demonstrated that GPC purification reliably removes small molecules such as excess precursor and weakly associated ligands for other metal chalcogenide and pnictide nanocrystals.[13,22,23] In smaller PbS QDs, this is also the case; however, in the case of the largest PbS QD samples, a population of free or weakly associated ligands remains even after multiple cycles of GPC purification (Figure 3).

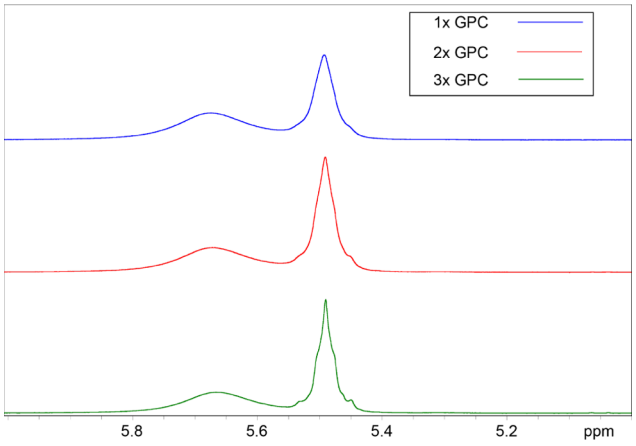

Figure 3. ^{1}H NMR of olefin region for large PbS QDs after multiple purification cycles via GPC.

Diffusion ordered spectroscopy (DOSY) was used to probe the two ligand populations and, in particular, to evaluate whether the remaining "unbound" feature, whose chemical shift and peak shape are comparable to free $Pb(OA)_2$ and oleic acid in the same solvent, could represent a population noncovalently bound (physisorbed) to the QDs. In fact, as can be seen in Figure S5, the two olefin peaks in the purified QD sample have distinct diffusion coefficients. The species responsible for the narrower olefin peak diffuses much more rapidly, indicating a smaller effective hydrodynamic diameter. However, the diffusion coefficient is slower than that of free oleic acid and is closer to that of $Pb(OA)_2$ (Figure S5). As the peak also appears for more strictly aprotic preparations described below, we assign the narrow peak to equivalents of $Pb(OA)_2$. In principle, GPC should accomplish dilution and separation of freely diffusing small molecules, and indeed removal of $Pb(OA)_2$ is accomplished for the smaller PbS QD samples in toluene. The persistence of the narrow peak following GPC for large-diameter QDs suggests a contribution from a weakly associated layer that is stabilized on the surface of larger-diameter PbS QDs at equilibrium. We note that the absorbance spectra before and after purification show no shift in the 1s absorbance peak (Figure S1), indicating the narrow peak cannot come from continued erosion of the PbS lattice.

Variable temperature (VT) NMR was used to probe this distribution of OA signals further and investigate the reversibility of the reaction between the two populations (Figure 4A). The temperature range of −20 to 40 °C was used, and over that range, integration of the two peaks shows a shift toward the narrower peak at higher temperature: the

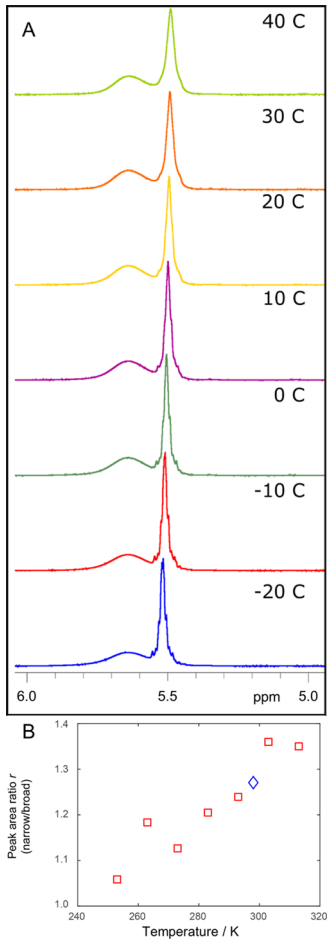

Figure 4. Variable-temperature ^{1}H NMR of large (6.12 nm) PbS QDs. (A) Detail of olefin resonance as a function of temperature. (B) Ratio r of peak integrals associated with narrow and broad olefin resonances in part A, respectively. Red squares represent measurements taken on heating from 253 K; blue diamond indicates a final measurement on return to room temperature.

percentage of "free" ligand increases from 51 to 57%. This change is indeed reversible, as cooling back to room temperature reverts the free ligand population to the initial 56%. Furthermore, there were no apparent changes in the absorbance spectra (Figure S7) to indicate any net changes to the particles after the thermal cycling in VT-NMR.

When Kessler and Dempsey looked at the reactive displacement of $Pb(OA)_2$ from the surface of PbS QDs on exposure to tetramethylethylenediamine (TMEDA), a nucleophilic (L-type) ligand,[11] they found that the extent of displacement correlates with faceting differences in differing sizes of PbS QDs, and also that the displaced TMEDA-$Pb(OA)_2$ adduct was in dynamic exchange with $Pb(OA)_2$ equivalents remaining at the surface. Here, we find that $Pb(OA)_2$ is labile on the largest-size PbS QDs even in the absence of a chelating ligand, with a shift to a less strongly interacting form at higher temperatures. However, in toluene solvent, at least a portion of this free $Pb(OA)_2$ population is retained in association with the QD surface.

We used quantitative ^{1}H NMR to compare large-diameter samples purified by GPC in toluene (following initial precipitation from the ODE growth solvent as described above) and by a second or third PR cycle in which acetone was added as the antisolvent and QDs were redispersed in toluene

https://dx.doi.org/10.1021/acs.chemmater.0c02024
Chem. Mater. 2020, 32, 6588−6594

(Figure S6). The narrow peak persisted following the PR cycles, though its relative intensity was greatly diminished compared to the GPC case, even though PR was less effective than GPC in removing residual ODE solvent. The equivalency of strongly bound OA (broad peak) per QD decreased very slightly in the PR cases, while the reversible shift toward the narrow peak at elevated temperature was maintained. These results indicate that large-diameter PbS QDs stabilize a weakly associated $Pb(OA)_2$ species in toluene that is partially disrupted by exposure to a more polar solvent environment during precipitation with acetone. We note that Grisorio et al. examined equilibrium among oleate-capped PbS QDs and solution-phase species, and found that effective diffusion constants for oleate species were larger in more polar solvents such as $CDCl_3$.[8] They also noted that the addition of $Pb(OA)_2$ precursor to 4.8 nm QDs in toluene yielded a distinct olefin resonance that exhibited dynamic exchange with the strongly bound broad peak. Our VT NMR on the 3× PR sample (Figure S6) indicates that this dynamic exchange can cause a distinct peak for weakly interacting $Pb(OA)_2$ to become unresolved within the broad OA resonance at higher temperatures. This labile character of $Pb(OA)_2$ ligands on larger-diameter QDs could contribute to difficulties in precisely determining ligand densities. However, when the peaks can be resolved, we see a consistent number of strongly bound OA equivalents among various purification methods.

From the VT-NMR data, we can in principle calculate a standard enthalpy change ΔH from a Van't Hoff plot of $\ln(K)$ versus $1/T$, where K is the equilibrium constant describing dissociation of $Pb(OA)_2$ from strongly bound sites. A lower bound on the total number of strong binding sites is the number occupied at the lowest temperature studied. However, efforts to assign K for a Langmuir-like isotherm from VT-NMR data predicted a larger variation in the extent of dissociation with concentration than was actually observed on further dilution in toluene. This is unsurprising because the product of the reaction is not (entirely) a freely diffusing species but remains in a weakly associated layer. A simple model in which the ratio r between narrow and broad peak contributions is taken to be the equilibrium constant gave $\Delta H = 2.5 \pm 0.4$ kJ/mol for the data in Figure 4.

Previous work on oleate-capped PbS QDs has proposed a significant role for water and/or hydroxide in terminating the surface and mediating dynamic equilibrium between free and bound ligand species, though this has not been studied in detail as a function of size. In particular, it was shown that in a Hines synthesis, in which the $Pb(OA)_2$ precursor is formed by the decomposition of PbO with oleic acid, the water evolved in this step is not completely removed and the precursor exists as a dimer of lead carboxylate hydrate. It has been proposed that this hydrate leads to a combination of hydroxide and oleate passivation on the surface of PbS.[21,24] This ligand passivation, in combination with excess precursors in the solution, has in turn been proposed as the basis for the observed dynamic ligand passivation in PbS QDs made from the Hines synthesis.[8] We did not observe evidence for a hydroxide stretch by FTIR spectroscopy of the GPC-purified samples (Figure S3). A ^1H NMR signal at ~0.5 ppm attributed to H_2O could be observed in some samples but was easily removed by activated 4 Å molecular sieves or GPC in an anhydrous solvent under an inert atmosphere. However, to investigate the possible influence of water on the ligand passivation, we chose to prepare PbS QDs using strictly anhydrous $Pb(OA)_2$ based on work from Hendricks et al.[17] Using this anhydrous $Pb(OA)_2$ to synthesize PbS quantum dots, we still find that two oleate species are observed after GPC purification for QDs of the larger radius (Figure S8). Therefore, it is unlikely that the observed dynamic oleate passivation is a consequence of hydroxide termination at the surface, but as discussed below, adventitious water does influence PbS QD growth via the Hines method.

Influence of Adventitious Water on PbS QD Growth. During the synthesis of the anhydrous PbS QDs, we observed that under similar reaction conditions, the resulting nanocrystals were consistently smaller in size compared to those using the "normal" Hines synthetic method (Figure 5). Specifically,

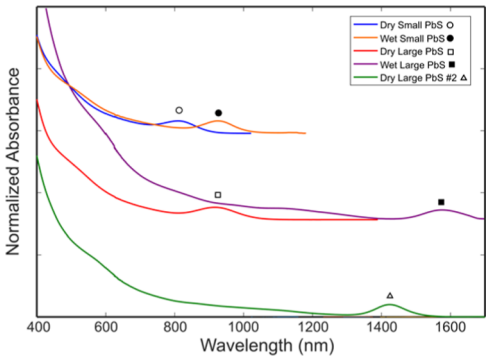

Figure 5. Normalized absorbance spectra of PbS made from normal and anhydrous lead oleate precursors. Spectra are displaced along the y-axis.

as described in detail by Zhang et al., the temperature and precursor concentrations in the Hines method can be varied to control the size of the QD product.[5] We found that for various representative sets of conditions, the "dry" method produced smaller particles, with larger effective band gaps, than did the normal method. This change occurred without any significant difference in the overall synthetic yield for PbS formula units in the reactions as determined by absorbance. Only by further increasing the concentration of $Pb(OA)_2$ were we able to make the larger-diameter "dry" sample shown in Figure 5 and used in the dynamic equilibrium comparison described above. Theoretical work from Stevenson et al. highlighted the importance that water played in the reaction mechanism of PbS in a Hines synthesis.[24] Their calculations show that in this reaction, $Pb(OA)_2$ is in the form of a dimer stabilized by hydrogen bonds with water. This dimer is the precursor that then reacts with $(TMS)_2S$ to form PbS monomers: the precursor to PbS QD nucleation. It has been shown for a variety of nanocrystal systems that precursor reactivity regulates size and concentration of the resultant nanocrystals.[25−27] Increasing the precursor reactivity leads to an increased monomer supply that leads to a higher concentration of smaller nanocrystals. Therefore, the different observed QD sizes can be explained by the increased reactivity of the $Pb(OA)_2$ in the absence of water-assisted dimerization as is the case in a typical Hines synthesis.

CONCLUSIONS

We have shown here that GPC purification in toluene provides a highly repeatable route to separate PbS QDs from small molecule impurities including a residual solvent. For smaller QDs of less than about 4 nm in diameter, GPC conveniently

https://dx.doi.org/10.1021/acs.chemmater.0c02024
Chem. Mater. 2020, 32, 6588−6594

yields QDs that are stable with a low free ligand concentration, such that ligand ratios and densities can be described precisely. As a purely size-based separation method, GPC tends to preserve nanoscale assemblies found in the elution solvent, and GPC purification has revealed that for larger PbS QDs in toluene, this can include a weakly associated form of lead oleate. This layer exists in a dynamic equilibrium with a more strongly bound form that has a well-defined number of binding sites. This weakly associated form is also observed in QDs synthesized from anhydrous precursors. Precipitation with acetone was able to partially remove the weakly interacting population, but the dynamic equilibrium is maintained suggesting that colloidally stable samples in this size range may require a measurable concentration of $Pb(OA)_2$ at equilibrium. Furthermore, the anhydrous synthesis reiterates recent findings as to the PbS QD reaction mechanism where removal of water destabilizes the hydrogen-bonded lead oleate dimer, creating a more reactive species, and consequently rapid nucleation with limited growth.

For use in devices, free (and bound) long-chain ligands such as oleates are generally to be removed through ligand exchange, either through the treatment of films in the solid state or preferably through solution-phase ligand exchange reactions.[28] We have shown that GPC purification results in stable PbS QD solutions with native lead oleate surface coordination. These purified samples can be utilized to make devices, as we have recently demonstrated in the formation of photovoltaic junctions between PbS QDs and wide-band-gap silicon carbide substrates.[15] However, the results shown here also indicate that the presence of free oleates may be inevitable in the case of colloidally stable stock solutions of large (>∼4 nm) PbS QDs. Efforts to remove these through aggressive cleaning steps could be detrimental, as equilibrium is re-established with more strongly bound oleates. Optimized GPC and/or PR solvent conditions could aid in isolating large-diameter QD samples with highly consistent ligand populations and associated chemical and electronic properties.

■ ASSOCIATED CONTENT

Supporting Information

The Supporting Information is available free of charge at https://pubs.acs.org/doi/10.1021/acs.chemmater.0c02024.

Anhydrous lead oleate reaction scheme, as well as Figures S1−S8 containing additional absorbance, TGA, and NMR spectra (PDF)

■ AUTHOR INFORMATION

Corresponding Author

Andrew B. Greytak − *Department of Chemistry and Biochemistry, University of South Carolina, Columbia, South Carolina 29208, United States;* orcid.org/0000-0001-8978-6457; Email: greytak@sc.edu

Authors

Adam Roberge − *Department of Chemistry and Biochemistry, University of South Carolina, Columbia, South Carolina 29208, United States;* orcid.org/0000-0002-2633-6755

John H. Dunlap − *Department of Chemistry and Biochemistry, University of South Carolina, Columbia, South Carolina 29208, United States;* orcid.org/0000-0002-0045-3603

Fiaz Ahmed − *Department of Chemistry and Biochemistry, University of South Carolina, Columbia, South Carolina 29208, United States;* orcid.org/0000-0002-6977-3672

Complete contact information is available at: https://pubs.acs.org/10.1021/acs.chemmater.0c02024

Notes

The authors declare no competing financial interest.

■ ACKNOWLEDGMENTS

This work was supported by the US NSF, through grant CHE-MSN 1613388 and in part by OIA-1655740. Additionally, A.R. and J.H.D. acknowledge NSF IGERT fellowships through grant 1250052. We thank Dr. Perry Pellechia for assistance in performing and interpreting VT-NMR experiments.

■ REFERENCES

(1) Kang, I.; Wise, F. W. Electronic Structure and Optical Properties of PbS and PbSe Quantum Dots. *J. Opt. Soc. Am. B* **1997**, *14*, 1632−1646.

(2) Kovalenko, M. V.; Manna, L.; Cabot, A.; Hens, Z.; Talapin, D. V.; Kagan, C. R.; Klimov, V. I.; Rogach, A. L.; Reiss, P.; Milliron, D. J.; Guyot-Sionnnest, P.; Konstantatos, G.; Parak, W. J.; Hyeon, T.; Korgel, B. A.; Murray, C. B.; Heiss, W. Prospects of Nanoscience with Nanocrystals. *ACS Nano* **2015**, *9*, 1012−1057.

(3) Sargent, E. H. Colloidal Quantum Dot Solar Cells. *Nat. Photonics* **2012**, *6*, 133−135.

(4) Hines, M. A.; Scholes, G. D. Colloidal PbS Nanocrystals with Size-Tunable Near-Infrared Emission: Observation of Post-Synthesis Self-Narrowing of the Particle Size Distribution. *Adv. Mater.* **2003**, *15*, 1844−1849.

(5) Zhang, J.; Crisp, R. W.; Gao, J.; Kroupa, D. M.; Beard, M. C.; Luther, J. M. Synthetic Conditions for High-Accuracy Size Control of PbS Quantum Dots. *J. Phys. Chem. Lett.* **2015**, *6*, 1830−1833.

(6) Moreels, I.; Justo, Y.; De Geyter, B.; Haustraete, K.; Martins, J. C.; Hens, Z. Size-Tunable, Bright, and Stable PbS Quantum Dots: A Surface Chemistry Study. *ACS Nano* **2011**, *5*, 2004−2012.

(7) Dong, C.; Liu, S.; Barange, N.; Lee, J.; Pardue, T.; Yi, X.; Yin, S.; So, F. Long-Wavelength Lead Sulfide Quantum Dots Sensing up to 2600 Nm for Short-Wavelength Infrared Photodetectors. *ACS Appl. Mater. Interfaces* **2019**, *11*, 44451−44457.

(8) Grisorio, R.; Debellis, D.; Suranna, G. P.; Gigli, G.; Giansante, C. The Dynamic Organic/Inorganic Interface of Colloidal PbS Quantum Dots. *Angew. Chem., Int. Ed.* **2016**, *55*, 6628−6633.

(9) Beygi, H.; Sajjadi, S. A.; Babakhani, A.; Young, J. F.; van Veggel, F. C. J. M. Surface Chemistry of As-Synthesized and Air-Oxidized PbS Quantum Dots. *Appl. Surf. Sci.* **2018**, *457*, 1−10.

(10) Weir, M. P.; Toolan, D. T. W.; Kilbride, R. C.; Penfold, N. J. W.; Washington, A. L.; King, S. M.; Xiao, J.; Zhang, Z.; Gray, V.; Dowland, S.; Winkel, J.; Greenham, N. C.; Friend, R. H.; Rao, A.; Ryan, A. J.; Jones, R. A. L. Ligand Shell Structure in Lead Sulfide−Oleic Acid Colloidal Quantum Dots Revealed by Small-Angle Scattering. *J. Phys. Chem. Lett.* **2019**, *10*, 4713−4719.

(11) Kessler, M. L.; Dempsey, J. L. Mapping the Topology of PbS Nanocrystals through Displacement Isotherms of Surface-Bound Metal Oleate Complexes. *Chem. Mater.* **2020**, *32*, 2561−2571.

(12) Hassinen, A.; Moreels, I.; De Nolf, K.; Smet, P. F.; Martins, J. C.; Hens, Z. Short-Chain Alcohols Strip X-Type Ligands and Quench the Luminescence of PbSe and CdSe Quantum Dots, Acetonitrile Does Not. *J. Am. Chem. Soc.* **2012**, *134*, 20705−20712.

(13) Shen, Y.; Roberge, A.; Tan, R.; Gee, M. Y.; Gary, D. C.; Huang, Y.; Blom, D. A.; Benicewicz, B. C.; Cossairt, B. M.; Greytak, A. B. Gel Permeation Chromatography as a Multifunctional Processor for Nanocrystal Purification and On-Column Ligand Exchange Chemistry. *Chem. Sci.* **2016**, *7*, 5671−5679.

(14) Shen, Y.; Gee, M. Y.; Greytak, A. B. Purification Technologies for Colloidal Nanocrystals. *Chem. Commun.* **2017**, *53*, 827−841.

(15) Kelley, M. L.; Letton, J.; Simin, G.; Ahmed, F.; Love-Baker, C. A.; Greytak, A. B.; Chandrashekhar, M. V. S. Photovoltaic and Photoconductive Action Due to PbS Quantum Dots on Graphene/SiC Schottky Diodes from NIR to UV. *ACS Appl. Electron. Mater.* **2020**, *2*, 134−139.
(16) Kroupa, D. M.; Arias, D. H.; Blackburn, J. L.; Carroll, G. M.; Granger, D. B.; Anthony, J. E.; Beard, M. C.; Johnson, J. C. Control of Energy Flow Dynamics between Tetracene Ligands and PbS Quantum Dots by Size Tuning and Ligand Coverage. *Nano Lett.* **2018**, *18*, 865−873.
(17) Hendricks, M. P.; Campos, M. P.; Cleveland, G. T.; Plante, I. J.-L.; Owen, J. S. A Tunable Library of Substituted Thiourea Precursors to Metal Sulfide Nanocrystals. *Science* **2015**, *348*, 1226−1230.
(18) Moreels, I.; Lambert, K.; Smeets, D.; De Muynck, D.; Nollet, T.; Martins, J. C.; Vanhaecke, F.; Vantomme, A.; Delerue, C.; Allan, G.; Hens, Z. Size-Dependent Optical Properties of Colloidal PbS Quantum Dots. *ACS Nano* **2009**, *3*, 3023−3030.
(19) Carey, G. H.; Abdelhady, A. L.; Ning, Z.; Thon, S. M.; Bakr, O. M.; Sargent, E. H. Colloidal Quantum Dot Solar Cells. *Chem. Rev.* **2015**, *115*, 12732−12763.
(20) Choi, H.; Ko, J.-H.; Kim, Y.-H.; Jeong, S. Steric-Hindrance-Driven Shape Transition in PbS Quantum Dots: Understanding Size-Dependent Stability. *J. Am. Chem. Soc.* **2013**, *135*, 5278−5281.
(21) Zherebetskyy, D.; Scheele, M.; Zhang, Y.; Bronstein, N.; Thompson, C.; Britt, D.; Salmeron, M.; Alivisatos, P.; Wang, L.-W. Hydroxylation of the Surface of PbS Nanocrystals Passivated with Oleic Acid. *Science* **2014**, *344*, 1380−1384.
(22) Shen, Y.; Gee, M. Y.; Tan, R.; Pellechia, P. J.; Greytak, A. B. Purification of Quantum Dots by Gel Permeation Chromatography and the Effect of Excess Ligands on Shell Growth and Ligand Exchange. *Chem. Mater.* **2013**, *25*, 2838−2848.
(23) Roberge, A.; Stein, J. L.; Shen, Y.; Cossairt, B. M.; Greytak, A. B. Purification and In Situ Ligand Exchange of Metal-Carboxylate-Treated Fluorescent InP Quantum Dots via Gel Permeation Chromatography. *J. Phys. Chem. Lett.* **2017**, 4055−4060.
(24) Stevenson, J. M.; Ruttinger, A. W.; Clancy, P. Uncovering the Reaction Mechanism Initiating the Nucleation of Lead Sulfide Quantum Dots in a Hines Synthesis. *J. Mater. Chem. A* **2018**, *6*, 9402−9410.
(25) Owen, J. S.; Chan, E. M.; Liu, H.; Alivisatos, A. P. Precursor Conversion Kinetics and the Nucleation of Cadmium Selenide Nanocrystals. *J. Am. Chem. Soc.* **2010**, *132*, 18206−18213.
(26) Hendricks, M. P.; Campos, M. P.; Cleveland, G. T.; Jen-La Plante, I.; Owen, J. S. A Tunable Library of Substituted Thiourea Precursors to Metal Sulfide Nanocrystals. *Science* **2015**, *348*, 1226−1230.
(27) Vela, J. Molecular Chemistry to the Fore: New Insights into the Fascinating World of Photoactive Colloidal Semiconductor Nanocrystals. *J. Phys. Chem. Lett.* **2013**, *4*, 653−668.
(28) Kirmani, A. R. Commercializing Colloidal Quantum Dot Photovoltaics. *MRS Bull.* **2019**, *44*, 524−525.

https://dx.doi.org/10.1021/acs.chemmater.0c02024
Chem. Mater. 2020, 32, 6588−6594